Original Article

JCBFM

Journal of Cerebral Blood Flow & Metabolism
0(0) 1–12

DOI: 10.1177/0271678X251358979
journals.sagepub.com/home/jcbfm
Sage

Characterizing pre- and post-operative cerebral blood flow and transit time in pediatric moyamoya patients using multi-delay ASL and DSC MRI

Moss Y Zhao[1,2], Sasha Alexander[1], Chris Antonio Lopez[1], Helena Zhang[3], Gabriella Morton[1], Rui Duarte Armindo[3], Kristen W Yeom[3], Elizabeth Tong[3], Bruno P Soares[3], Sarah Lee[4], Michael Moseley[3] and Gary K Steinberg[1,4]

Abstract

Cerebral blood flow (CBF) and transit time are essential biomarkers for assessing brain health. While dynamic susceptibility contrast (DSC) MRI has been widely applied to measure these metrics, it is limited in the pediatric population due to the need for contrast agents. Arterial spin labeling is a non-invasive and quantitative MR modality, and multi-delay ASL can measure CBF and transit time simultaneously. Although multi-delay ASL has been used in adult neuroimaging studies, its application in children requires investigation. Moyamoya disease, a progressive steno-occlusive cerebrovascular disorder, often manifests in childhood. In this work, we present a cohort study that examines multi-delay ASL and DSC MRI to characterize vascular hemodynamics in 22 pediatric patients. We evaluate CBF and transit time in different brain regions before and after revascularization surgeries. Results show that revascularization significantly increased CBF by 24% and 7.6%, respectively, as measured by ASL and DSC; it also significantly decreased transit time by 12% and 15%, indicating improved hemodynamics and metabolism. ASL and DSC results also showed significantly positive correlations in all brain regions. Thus, revascularization improved hemodynamics in pediatric moyamoya patients and shows that multi-delay ASL can effectively characterize CBF and transit time in the pediatric population.

Keywords

Cerebral blood flow, arterial transit time, arterial spin labeling, moyamoya disease, dynamic susceptibility contrast

Received 15 January 2025; Revised 20 June 2025; Accepted 30 June 2025

Introduction

Moyamoya disease is a progressive, non-acute inflammatory cerebrovascular disorder that results in stenosis or occlusion in the supraclinoid segment of the internal carotid artery (ICA), proximal anterior cerebral artery (ACA), and proximal middle cerebral artery (MCA), conferring a higher risk for strokes or transient ischemic attacks.[1] Many moyamoya patients begin having neurological symptoms during childhood, and the condition deteriorates with aging.[2] Revascularization (or bypass) procedures can restore the blood supply in regions affected by vasculopathy, leading to stroke prevention and improved neurological and neurocognitive outcomes.[3–6]

Cerebral blood flow (CBF) is a hemodynamic metric that quantifies the amount of arterial blood delivered to brain tissues.[7] Since CBF reflects brain metabolism and tissue health,[8] it has become a key clinical biomarker to diagnose cerebrovascular diseases and evaluate treatment outcomes for patients with

[1]Department of Neurosurgery and Stanford Stroke Center, Stanford University, Stanford, CA, USA
[2]Maternal and Child Health Research Institute, Stanford University, Stanford, CA, USA
[3]Department of Radiology, Stanford University, Stanford, CA, USA
[4]Department of Neurology, Stanford University, Stanford, CA, USA

Corresponding author:
Gary K Steinberg, Bernard and Ronni Lacroute-William Randolph Hearst Professor of Neurosurgery and the Neurosciences, Department of Neurosurgery and Stanford Stroke Center, Stanford University School of Medicine, 1201 Welch Road (P305), Stanford, CA 94305-5327, USA.
Email: gsteinberg@stanford.edu

neurological diseases.[9] Transit time is another hemodynamic value that has gained considerable importance in characterizing cerebrovascular diseases; it can directly characterize blood circulation and identify vasculopathies resulting in arterial stenosis and occlusion.[10,11] For example, arterial transit time and time-to-maximum both reflect delayed blood arrival and have clinical utility in evaluating cerebral circulation and vascular health. While measured using different imaging techniques, they serve as complementary indicators of hemodynamic status. Dynamic susceptibility contrast (DSC) MRI—with intravenously administered gadolinium as the contrast agent—is a commonly used clinical imaging modality with commercially available tools to measure CBF and transit time (such as mean transit time, MTT as well as time to maximum, Tmax), particularly in adult populations and in conditions where contrast use is clinically justified.[12] In pediatric patients, a standardized scoring system based on DSC-derived time-to-peak was proposed to evaluate indirect revascularization in pediatric moyamoya patients, showing that preoperative perfusion status could predict surgical outcomes.[13] Also, DSC MRI was used to assess posterior cerebral artery involvement following anterior bypass surgery, highlighting its diagnostic value in postoperative monitoring.[14] While DSC MRI has been widely applied in stroke imaging protocols,[15] the use of intravenous contrast has limited application in the routine pediatric population. For example, due to immature renal function in children, acute adverse reactions after the use of MR contrast agents have been reported.[16,17] Arterial spin labeling (ASL) is a non-invasive and quantitative MRI technique that uses arterial blood as the endogenous tracer to characterize CBF.[18] ASL with a single post-labeling delay, or single-delay ASL, has been extensively employed in clinical neuroimaging.[19] However, multi-delay ASL can simultaneously measure CBF and arterial transit time (ATT).[20] Several studies have demonstrated the strengths of multi-delay ASL in evaluating vascular hemodynamics in adult patients with cerebrovascular diseases.[21] However, the effectiveness of multi-delay ASL in children remains to be elucidated. In particular, comparing ASL with commonly used clinical perfusion MRI techniques, such as DSC, in the pediatric population would provide vital evidence to reduce the need for IV gadolinium-based contrast agents and enhance pediatric neuroimaging. Additionally, while several studies have demonstrated improved perfusion in moyamoya patients after revascularization, the effectiveness of advanced imaging techniques, such as multi-delay ASL,[4–6] in evaluating pediatric hemodynamics after neurosurgery remains understudied, particularly in direct comparison to conventional DSC MRI before and after neurosurgery.

This study aims to evaluate CBF and transit time (including ATT and Tmax) in pediatric moyamoya patients using multi-delay ASL and DSC MRI, and to compare hemodynamic changes before and after bypass surgery across both imaging modalities.

Materials and methods

Study overview

The study complied with the regulations of the Institutional Review Board of Stanford University. All procedures were conducted in accordance with the Declaration of Helsinki.[22] This prospective cohort study was conducted between January 2021 and January 2024. A total of 26 pediatric patients initially met the inclusion criteria during the study period; however, four patients were excluded because they did not participate in the 6-month follow-up post-surgical imaging session. As a result, 22 patients (5 males and 17 females, between 3 and 18 years old) were included in the final analysis. Written informed consent was obtained from all patients and caregivers. These patients had either unilateral or bilateral moyamoya disease. They were treated by extracranial to intracranial revascularization surgery (superficial temporal artery to middle cerebral artery [STA-MCA] bypass) at our institution. Our cohort includes pediatric patients with moyamoya vasculopathy, defined by characteristic radiographic findings and neurological symptoms. Inclusion criteria were a confirmed diagnosis of moyamoya disease (untreated by bypass) based on digital subtraction angiography (DSA). Vasculopathies were graded on DSA scans. Exclusion criteria included kidney function impairment (glomerular filtration rate <40 ml/min), history of traumatic brain injury or head trauma, and contraindications to MRI. In brief, STA-MCA bypass was performed by connecting the frontal or temporal branch of STA and the M4 segment of MCA under mild hypothermia (33–35°C).[23] For patients with bilateral vasculopathy requiring bypass on both sides of the brain, two surgeries were performed; they were separated by at least a week but less than three months.

Patient information

Table 1 shows both the demographic information and the condition of vasculopathy of the pediatric moyamoya cohort. Among the 22 patients enrolled, there were 17 females and five males. A total of 44 hemispheres were studied. Their age at the time of their first surgery ranged between 3 and 18 years, with a median value of 12 years. There were 12 Caucasians,

Table 1. Demographic information of the study cohort.

Parameter	Value
Number of patients	22 (5 males and 17 females)
Age at the time of surgery	3–18 years old. Median age: 12 years.
Race	12 Caucasians, 8 Asians, 1 Hispanic, 1 other[a]
Time between pre- and post-surgery scans	172–230 days. Median: 194 days

[a]Others include Pacific Islander and mixed race.

8 Asians, one Hispanic, and one patient of another race and/or ethnicity. The time between pre-surgery and post-surgery imaging ranged from 172 to 230 days, with a median of 194 days. Other clinical information can be found in Table S1 in Supplementary Materials.

MR imaging

MR imaging data were acquired using Discovery MR 750 3.0T MRI systems (GE Healthcare, Chicago, IL, USA) 1 week before and 6 months after revascularization surgery in each patient. All procedures were performed according to the Institutional Review Board (IRB) regulations of Stanford University and the Declaration of Helsinki. Our moyamoya MR protocol included the following sequences: T1-weighted, T2-weighted, FLAIR, DWI, MRA, multi-delay ASL, and DSC MRI. Specifically, the labeling plane of the multi-delay ASL was placed perpendicular to the ICA between C2 and C3 vertebrae with effective labeling duration = 550 msec; 7 post-labeling delays = 700, 1250, 1800, 2350, 2900, 3450, and 4000 msec, and Hadamard labeling technique. A proton density image (M0) and a coil sensitivity map were acquired for all ASL scans, with a saturation recovery acquisition using TR = 2000 ms and other readout parameters identical to the ASL sequence. The Hadamard labeling technique was implemented as a research sequence under an institutional agreement with GE Healthcare. DSC MRI was performed at the end of each imaging session using 0.1 mmol/kg of gadobenate dimeglumine (Multihance, Bracco, Milan, Italy) injected at a rate of 4 mL/s and a pre-delay of 18 s. The MRA was centered on the Circle of Willis, covering 40 mm in the superior-inferior direction. Other imaging acquisition parameters can be found in Table 2. Patients were instructed to refrain from food and beverages containing caffeine at least 6 hours before the MRI session.[24] Patients that received sedation during MR sessions always had sedation in both pre- and post-surgical scans. Propofol was used as the hypnotic agent due to its quick onset and recovery. Fasting was required for at least 6 hours before the imaging session. All MR data were de-identified after image reconstruction.

CBF and transit time measurements

Voxel-wise hemodynamic values were measured, including CBF and ATT from multi-delay ASL, as well as CBF and Tmax from DSC MRI. Specifically, CBF and ATT were calculated by fitting the general kinetic model to the ASL difference data using spatially variational Bayesian inference techniques implemented in the FSL tool BASIL (Bayesian Inference for Arterial Spin Labeling; compiles quantitative CBF images from ASL data).[25] The mean and standard deviation of the priors used in BASIL were 0 and 1000 for CBF (ml/100g/min), and 0.7 and 0.3 for ATT (seconds), respectively. Dispersion and macrovascular correction were not applied in the BASIL. The labeling efficiency was assumed to be 85%, and the blood-brain partition coefficient to be 90%.[26] Partial volume effects on the edge of the brain were corrected using the erosion and extrapolation method[27]; no additional partial volume correction was applied elsewhere in the brain. CBF and time to peak (Tmax, defined as the time to maximum of the tissue residue function) values were computed by deconvolution of the DSC data using RAPID® software (RapidAI, San Mateo, CA, USA).[28]

All hemodynamic maps were transformed from native space to the Montreal Neurological Institute (MNI) 152-2mm space to facilitate group comparison and statistical analysis using both linear and non-linear registration implemented in FSL.[29] Six flow territories (left ACA, right ACA, left MCA, right MCA, left PCA, and right PCA) were defined based on the Harvard-Oxford cortical and subcortical structural atlases.[30] The mean CBF and transit time values in each flow territory were computed. The location and severity of vasculopathy were assessed on preoperative DSA by board-certified neuroradiologists (co-authors of the study). Grading was performed bilaterally across the anterior, middle, and posterior cerebral artery territories, using a system routinely applied in clinical practice. While this grading was based on expert clinical judgment and not a formalized scoring system, it is consistent with previously reported approaches in the literature.

Statistical analysis

All statistical tests were performed using MATLAB (Mathworks, Natick, MA, USA, version 2023a). The normality of the mean CBF and transit time values was confirmed using Kolmogorov–Smirnov tests before conducting statistical analyses.[31] Paired t-tests were performed to compare the mean values of CBF and

Table 2. Parameter values of MRI sequences.

Parameter	Unit	Value
MRA		
TR/TE	ms	23/2.6
Number of slices		180
Flip angle	degrees	15
Slice thickness	mm	1.2
Matrix		512×512
FOV	mm^2	220×220
Voxel size	mm^2	0.45×0.45
Scan duration	min	3:57
Multi-delay PCASL		
Labeling pulse shape		Hanning
Labeling pulse duration	ms	0.5
Labeling pulse spacing	ms	1.22
RF pulse strength	Gauss	0.018
Mean gradient strength	mT/m	0.7
Maximal gradient strength	mT/m	4.5
Bolus duration	ms	2000
TR/TE	ms	6484/10.53
PLD	ms	700, 1325, 1950, 2575, 3200
Acquisition matrix		4 spirals $\times$ 512 sampling points
NEX		1
Number of slices		36
FOV	cm^3	24
Acquisition voxelsize	mm	$5.77 \times 5.77 \times 4$
Reconstruction voxelsize	mm	$1.719 \times 1.719 \times 4$
Number of background suppression pulses		5
Scan duration	min	4:39
DSC		
TR/TE	ms	1800/40
NEX		1
Flip angle	degrees	60
Slice thickness	mm	5
Number of slices		24
FOV	cm	22×22
Matrix		128×128
Acquisition voxel size	mm	1.719×1.719
Scan duration	Min	2:28

transit time measured by multi-delay ASL, as well as DSC MRI, before and after bypass in regions affected by vasculopathy. The null hypothesis was that the value of these parameters was the same. A p-value <0.05 was considered statistically significant. Pearson correlation was performed to examine the correlation between hemodynamic values measured by multi-delay ASL and DSC MRI before and after surgery.

Results

Hemodynamic maps of an example patient

Figure 1 shows the hemodynamic maps of a 16-year-old female moyamoya patient. Occlusion at the left MCA can be seen based on the pre-surgery MRA scans in Figure 1(a). There are also extensive lenticulostriate collateral vessels near the occlusion site. The STA-MCA graft can be observed 6 months after the surgery. Regarding the CBF maps in Figure 1(b), decreased CBF at left MCA can be seen in the pre-surgery maps obtained by both ASL and DSC MRI. After surgery, the CBF in these regions increased towards the values on the right (healthy) side of the brain. Regarding the transit time maps in Figure 1(c), delayed ATT and Tmax at the left MCA regions due to occlusion can be seen in the pre-surgery maps acquired by ASL and DSC MRI, respectively. After revascularization, ATT in these regions decreased; the transit time was still longer than the healthy side of the brain. There was no evidence of brain infarction or white matter disease in this patient. As shown in

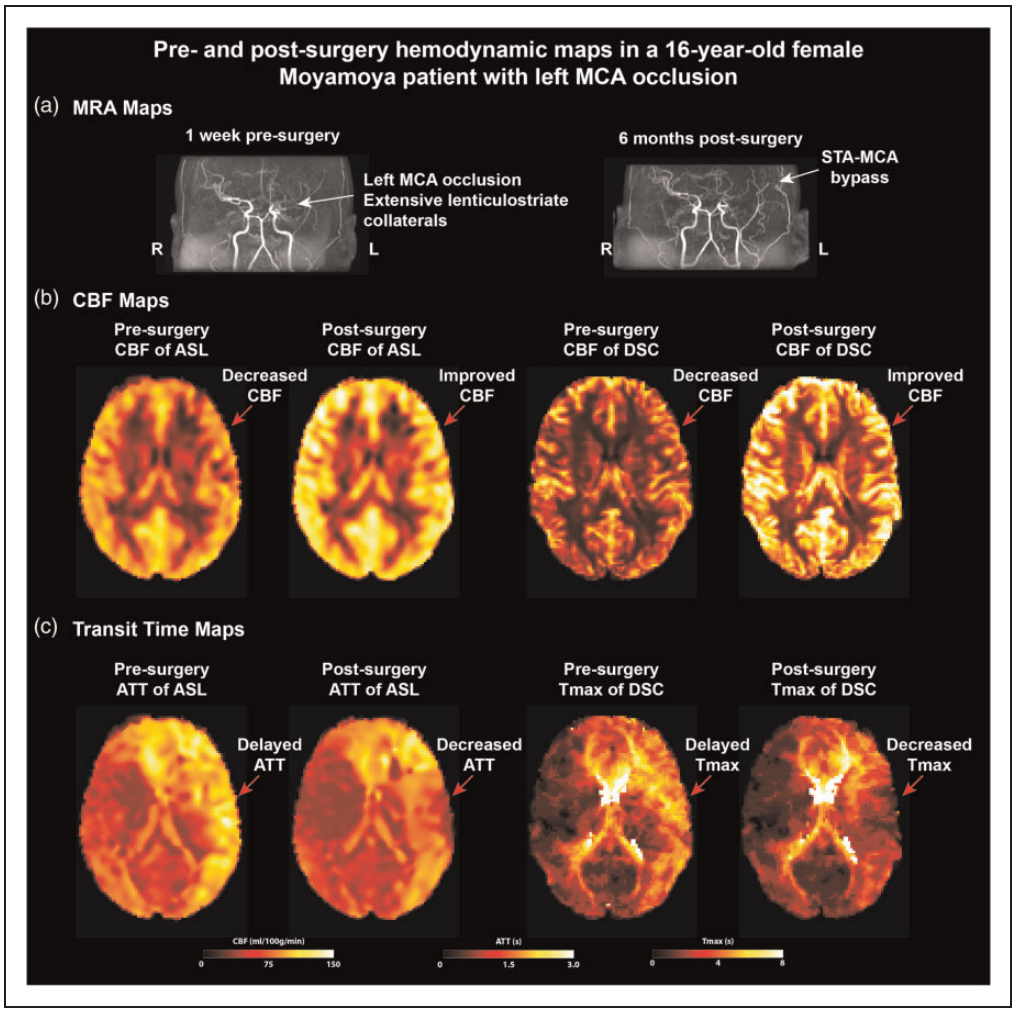

Figure 1. Pre- and post-surgery hemodynamic maps of a pediatric moyamoya patient with left MCA occlusion. (a) The pre-surgery MRA shows occlusion at the left MCA with lenticulostriate collateral vessels, and the post-surgery MRA displays the STA-MCA graft. (b) The pre-surgery ASL shows decreased CBF in the left MCA territory; CBF improved post-surgery. A similar trend can be seen in the CBF maps obtained by DSC MRI and (c) in the transit time maps, the pre-surgery ASL map shows delayed ATT in the left MCA region; ATT decreased (improved) post-surgery. Similar observations can be found in Tmax maps obtained by DSC MRI.

Table S2 in Supplementary Materials, asymmetry index of CBF increased; asymmetry index of ATT decreased; asymmetry index of Tmax decreased, consistent with improved hemodynamic balance.

CBF changes and correlations

Figure 2 shows the changes in mean CBF before and after surgery measured by multi-delay ASL and DSC MRI. For ASL measurements, mean CBF increased significantly after bypass surgery by $24\% \pm 29\%$ ($p < 0.01$) and $7.6\% \pm 12\%$ ($p = 0.04$) in regions affected by vasculopathy and healthy regions, respectively. Similarly, CBF obtained by DSC MRI showed a similar trend, whereby the increment after revascularization was $18\% \pm 24\%$ ($p < 0.01$) and $5.8\% \pm 9.9\%$ ($p = 0.04$) in regions affected by vasculopathy and healthy regions, respectively. This indicated improved blood perfusion in the areas affected by vasculopathy and healthy brain regions following the bypass surgery. Paired CBF changes can be found in Figure S1 and Figure S2 in the Supplementary Materials.

Figure 3 shows the correlation between CBF measured by ASL and DSC MRI. These two MRI techniques have a significant and positive correlation in both pre- and post-surgery conditions. Specifically, the correlation between CBF in regions with vasculopathy was higher than in healthy brain regions ($R^2 = 0.41$ vs. $R^2 = 0.24$, respectively). Bland-Altman analysis can be found in Figure S3 in the Supplementary Materials.

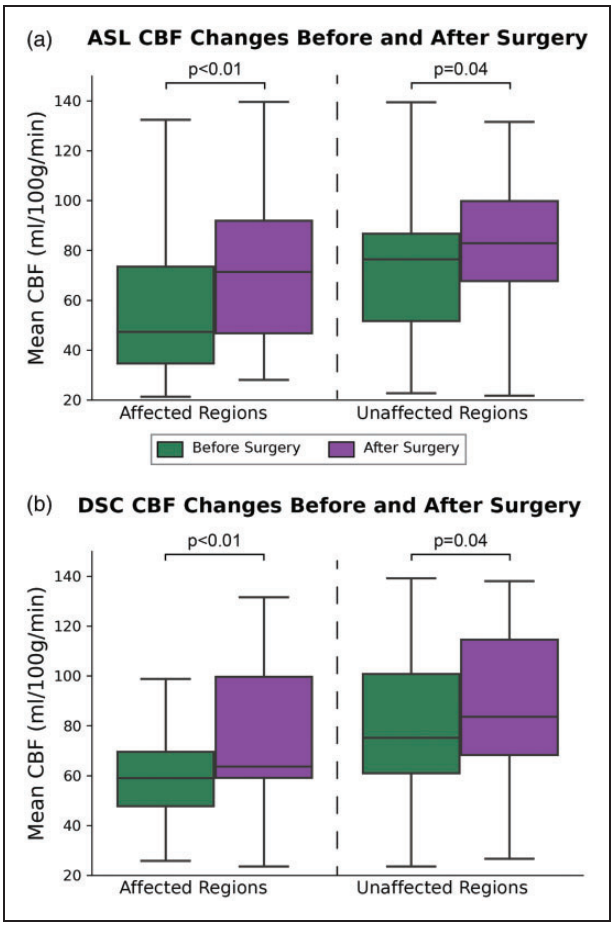

Figure 2. Box plots showing CBF changes before and after surgery. (a) CBF results measured by ASL MRI and (b) CBF results measured by DSC MRI. For both ASL and DSC results, mean CBF increased significantly after revascularization in both affected and healthy regions. Each box plot indicates, from top to bottom, the maximum, 75th, 50th, 25th percentiles, and minimum.

Transit time changes and correlations

Figure 4 illustrates the changes in transit time before and after surgery as measured by multi-delay ASL and DSC MRI. Overall, mean transit times (ATT and Tmax) reduced significantly by $12\% \pm 11\%$ ($p < 0.01$) and $15\% \pm 16\%$ ($p < 0.01$) measured by ASL and DSC, respectively, in regions affected by vasculopathy after surgery for the cohort; this implied that blood circulation improved due to the STA-MCA graft. In the areas without vasculopathy (healthy brain regions), no significant transit time changes were seen before and after surgery ($p = 0.29$ and $p = 0.68$ for ASL and DSC results, respectively). Paired ATT changes can be found in Figure S4 in Supplementary Materials; paired Tmax changes can be found in Figure S5 in the Supplementary Materials.

Figure 5 shows the correlation between transit time values measured by ASL and DSC MRI in the study cohort. Overall, a significant and positive correlation exists between ATT measured by ASL and Tmax measured by DSC MRI in pre- and post-surgery conditions. The correlation was higher in healthy regions than in regions affected by vasculopathy ($R^2 = 0.65$ vs. $R^2 = 0.49$, respectively).

Discussion

In this study, we evaluated vascular hemodynamics in a cohort of 22 pediatric moyamoya patients before and after revascularization using both multi-delay ASL and DSC MRI. Our analysis focused on three key perfusion parameters: cerebral blood flow (CBF), arterial transit time (ATT), and time-to-maximum (Tmax). We found that bypass surgery significantly increased CBF and decreased ATT and Tmax in regions affected by vasculopathy. Additionally, the observed significant correlation between ATT and Tmax supports the potential utility of multi-delay ASL as a non-invasive and quantitative technique for evaluating cerebrovascular health in pediatric patients after neurosurgery.

Impact of revascularization on CBF

We found that revascularization significantly increased CBF in both affected and healthy regions in this pediatric cohort. For both ASL and DSC MRI results, the effect size (or percentage of CBF change) in affected regions was larger than in the healthy regions. These data imply that revascularization significantly improves hemodynamics in regions with vasculopathy. By contrast, a previous study using single-delay ASL reported no significant change in baseline CBF in the ipsilateral MCA territory following bypass surgery in pediatric moyamoya patients.[32] These distinct results may reflect differences in imaging techniques. Our results also demonstrated the impact of revascularization on healthy brain regions of this pediatric cohort, whereby blood perfusion increased significantly after bypass surgery. This is distinctly different from previous studies evaluating blood perfusion in adult moyamoya patients, where blood perfusion did not increase after revascularization.[1,4,33] Our findings suggest that revascularization surgery in pediatric moyamoya patients improves circulation, not only in the affected regions but also in normal brain tissue. These data indicate that bypass surgeries positively affect overall cerebral autoregulation, benefiting these patients' brain function across affected and healthy areas. Our work has highlighted the potential systemic benefits of revascularization, suggesting that such surgeries help optimize brain function and improve cerebral health in

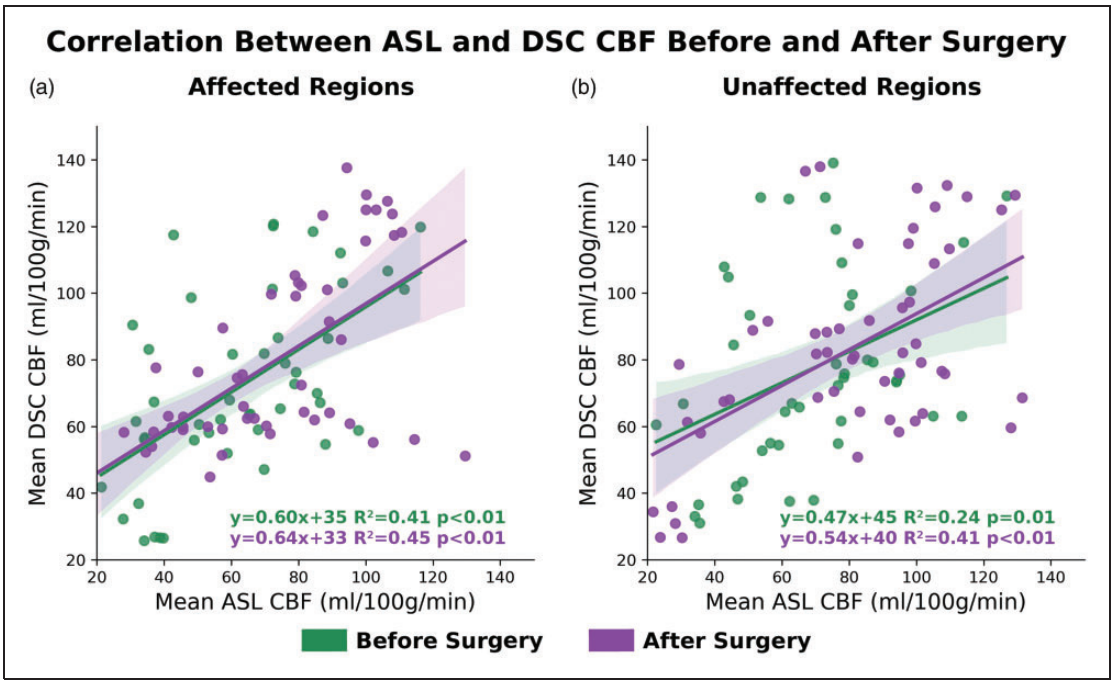

Figure 3. Correlation between CBF measured by ASL and DSC before and after surgery. (a) Results in regions affected by vasculopathy and (b) results in healthy or unaffected regions. Overall, significantly positive correlations can be found between ASL and DSC in both conditions. The correlation was higher in affected regions than healthy regions. The shaded area represents the 95% confidence interval.

pediatric moyamoya patients. Additionally, comparisons between our findings and previous studies should be made with caution, as differences in imaging techniques (e.g., single-delay vs. multi-delay ASL), region-of-interest definitions, and quantification methods can lead to variability in reported CBF changes following revascularization.

A common feature among the ASL and DSC CBF results was the broad range of CBF values measured by these two techniques. Specifically, this range was between 20 ml/100g/min to 140 ml/100g/min in either affected or healthy regions, similar to previous studies that reported a large range of pediatric CBF values.[34,35] This inter-subject difference may have two possible explanations: (1) the reproducibility of the imaging modalities was relatively low, causing large variabilities; (2) there is a significant variability of CBF within the pediatric population. We believe that variability in the pediatric patient population, including differences in age and brain development, likely plays a more substantial role than technical reproducibility alone. However, methodological factors, such as low SNR in ASL in low perfusion regions, sensitivity to transit time, and partial volume effects, may also contribute to both inter-subject variation and reproducibility. While it is beyond the scope of this study to address this intriguing question, a possible extension of our work is to investigate the normal range of pediatric CBF and the reproducibility of perfusion imaging techniques in a typical pediatric cohort. Accounting for effects due to age and sex may also enrich our understanding of how normal brain development influences hemodynamic changes in the pediatric population.

We also observed a crossover pattern in CBF measurements between ASL and DSC, whereby DSC tended to yield higher values in low-perfusion regions, while ASL produced higher values in high-perfusion areas. One possible explanation is that ASL may underestimate CBF in regions with prolonged arterial transit time caused by moyamoya vasculopathies, as labeled blood may not reach the tissue before image acquisition—despite our use of multi-delay sampling. By contrast, DSC may overestimate CBF in these same regions due to limitations in deconvolution under delayed bolus arrival. In high-flow regions, ASL benefits from full delivery of labeled spins, whereas DSC can underestimate flow due to contrast bolus saturation or signal loss from T2* effects. These technical and physiological differences may account for observations in the two perfusion imaging modalities.

Impact of revascularization on transit time

A key contribution from our work is to characterize transit time, defined as the time required for blood to travel from the labeling or bolus point to the tissue of

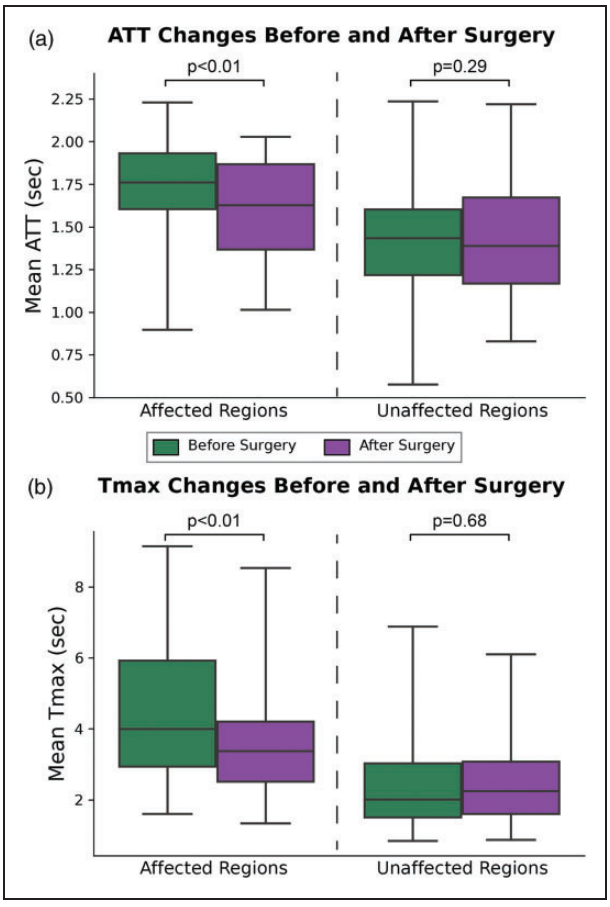

Figure 4. Box plots showing transit time changes before and after bypass surgery. (a) Mean ATT in regions affected by vasculopathy reduced significantly after bypass and (b) mean Tmax reduced significantly after bypass in regions affected by moyamoya vasculopathy. No significant transit time changes are found in healthy brain regions. Each box plot indicates, from top to bottom, the maximum, 75th, 50th, 25th percentiles, and minimum.

interest, using the standard DSC MRI in addition to our novel and non-invasive multi-delay ASL MRI in the pediatric population. Both techniques demonstrated a significant decrease in transit time after revascularization in regions affected by vasculopathy. This indicates improved blood circulation to regions usually supplied by stenosed or occluded moyamoya arteries through the STA-MCA graft. In contrast to the CBF results in the healthy brain regions, there was no significant change in transit time after surgery in healthy brain regions. A possible explanation could be that bypass surgeries did not alter the anatomy of the vasculature and underlying blood circulation within the healthy areas of the brain, causing transit time to be the same before and after surgery. Whilst the circulation remains unchanged after revascularization, it is possible that the cellular metabolism and functional activities improved, causing CBF to increase significantly after bypass through metabolic-vascular coupling. Since our work focuses on evaluating pediatric hemodynamics using ASL and DSC MRI, a more systematic investigation is warranted in future studies to characterize transit time variations in healthy brain tissues over time.

A key distinction between ATT (measured by ASL) and Tmax (measured by DSC MRI) lies in their physiological interpretation and the underlying signal modeling. ATT reflects the time for magnetically labeled arterial blood to travel from the labeling plane to the tissue of interest.[36] In contrast, Tmax represents the time-to-maximum of the residue function obtained from the deconvolution of the DSC signal, and is influenced by the arrival delay of the contrast bolus.[37] These differences may explain the variability observed between ATT and Tmax in our study. Despite the different modeling assumptions, the strong and positive correlation between ATT and Tmax suggests that both metrics capture complementary aspects of delayed perfusion. In moyamoya disease, where collateral circulation is common, dispersion can also significantly prolong Tmax values, especially in regions with slow blood flow.[38] While ATT is less affected by dispersion, it is influenced by technical factors such as the labeling plane and labeling strategy. In this study, the labeling plane was consistently placed between C2 and C3, and pseudo-continuous ASL with Hadamard-encoded multi-delay labeling was used across all patients, ensuring consistency in ATT estimation across flow territories and time points.

Comparing ASL and DSC MRI in characterizing pediatric hemodynamics

Prior studies have demonstrated the utility of DSC MRI in evaluating hemodynamic changes in moyamoya patients, supporting its role as a commonly used clinical perfusion modality.[39,40] Results obtained by ASL and DSC showed significant correlations in both pre- and post-surgery conditions. Specifically, in regions affected by vasculopathy, the correlation between CBF measured by ASL and DSC was higher in the pre-surgery condition than in post-surgery. Similar results can be observed in the correlation of transit time measurements. This finding differs from results observed in the adult population after surgery, whereby CBF in healthy brain regions did not change significantly after surgery.[4] A possible explanation is the unique and heterogeneous recovery from surgery, which may differ between children and adults, in addition to the normal brain development occurring among pediatric patients. A possible extension of the current study would be to explore variations in CBF and

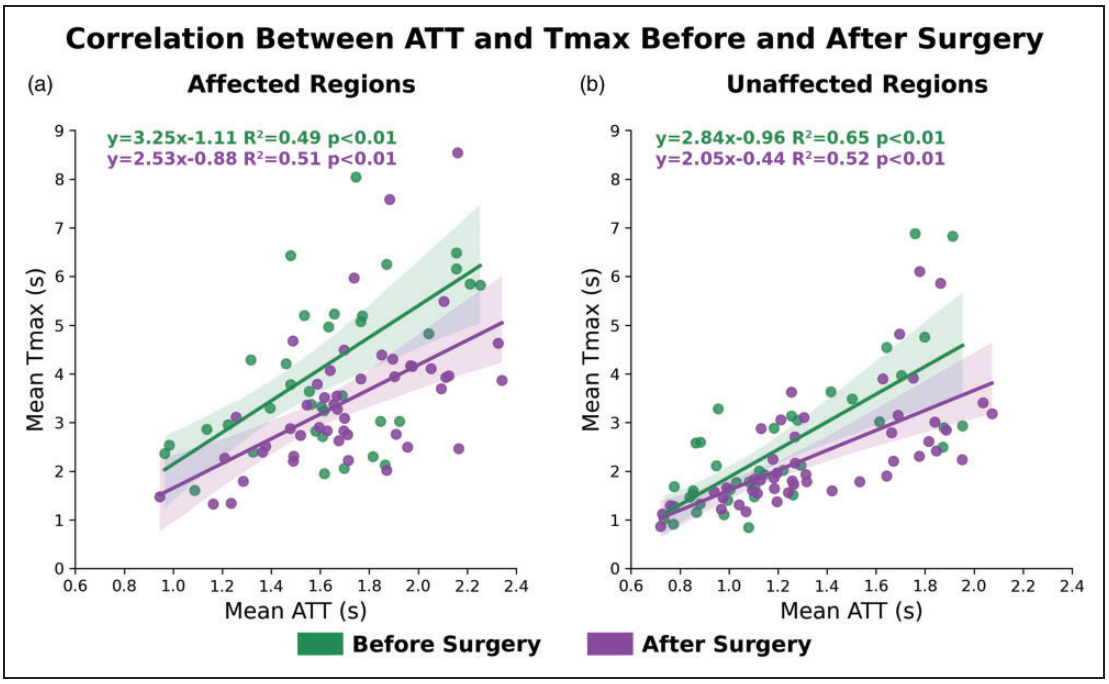

Figure 5. Correlation between mean ATT and Tmax measured by ASL and DSC MRI. Overall, significantly positive correlations between ATT and Tmax can be found in all conditions before and after surgery. (a) The correlation slightly increased after surgery in regions affected by vasculopathy and (b) the correlation decreased marginally after surgery in healthy regions. The shaded area represents the 95% confidence interval.

transit time across different ages during normal brain development in healthy children. Examining these global and regional changes would provide a more detailed understanding of hemodynamic changes in pediatric populations, potentially shedding light on age-related differences in brain maturation and offering insights into how these changes may impact overall brain function and development.

Our multi-delay ASL strategy also offers unique image acquisition and reconstruction advantages for pediatric neuroimaging. Although the total scanning time of the ASL technique was longer than that of DSC (5 minutes vs. 3.5 minutes, respectively), the total time needed to acquire these images was similar because DSC MRI requires the preparation of contrast agents, while ASL does not. Specifically, a trained MR technologist must calculate the amount of contrast agent to be injected and load it into the equipment. Also, an additional 18 seconds of pre-delay is required for each DSC MRI scan. None of these steps is needed for ASL MRI. While multi-delay ASL mitigates some of the limitations related to delayed arterial transit times, it may still underestimate perfusion in cases with extensive collateral flow or contributions from the external carotid artery, especially in advanced stages of moyamoya. Future studies using vessel-selective ASL may provide more detailed insights into collateral-specific hemodynamics.

Additionally, ASL can be performed repeatedly without the need for contrast agents, making it a favorable choice for treatment follow-ups and longitudinal studies for the pediatric population. Another advantage of ASL is in image quality. Specifically, DSC scans exhibit significant susceptibility artifacts near the frontal sinuses due to fast EPI readout methods.[41] This may cause challenges in analyzing imaging markers, such as CBF and Tmax, in the ACA territory, where vasculopathy is commonly found in patients with cerebrovascular diseases. On the contrary, ASL data has no susceptibility artifacts because a 3 D spiral readout is applied to acquire the label/control images.[42] This strategy ensures the same image quality in cortical regions and regions near the sinuses.

Limitations of the study

There are limitations in our study. One is that we did not enroll a control group consisting of healthy children to compare hemodynamic measurements using ASL and DSC MRI. The primary reason was due to the challenges involved in administering contrast agents to healthy children in neuroimaging studies. We attempted to resolve this challenge by demonstrating the correlation between ASL and DSC results in healthy brain regions. Our results showed significant and positive correlations between these two modalities.

Whilst there are also other perfusion imaging modalities, such as ^{15}O-water positron emission tomography (PET) and Xenon-133 single photon emission computed tomography (SPECT), an open experimental question is whether the different imaging modalities are more or less favorable than each other for pediatric neuroimaging. This may be addressed in future work using a similar experimental design in multi-center studies, including pediatric patients with different cerebrovascular diseases. While some patients in this cohort may overlap with those included in our prior studies presented only in conference abstracts, the current study aims to systematically evaluate pre- and post-operative CBF, ATT, and Tmax in pediatric moyamoya patients using both multi-delay ASL and DSC MRI. Our patient cohort included both idiopathic and syndromic cases of moyamoya, including two patients with Down syndrome. While the term 'moyamoya disease' is typically reserved for idiopathic cases,[43] we used this terminology throughout the manuscript for consistency. Our primary objective was to evaluate cerebrovascular hemodynamics using advanced imaging techniques in pediatric moyamoya vasculopathy, irrespective of underlying etiology. Future studies may explore whether imaging characteristics differ between idiopathic and syndromic subtypes. While sedation may affect hemodynamics in children, patients in our cohort who received sedation always had sedation in both pre- and post-surgical scans, making the effect of sedation on our data negligible. In this study, we observed a wide range of CBF values across patients, in both healthy and affected regions. While part of this variation may reflect true physiological differences, such as due to developmental variability, technical and methodological limitations should also be considered. These include the known sensitivity of ASL to reduced SNR in low-perfusion regions and partial volume effects. Future work is needed to elucidate the reproducibility of ASL and DSC in pediatric patients. This study employed a standard pediatric MNI template (as shown in Figure S6 in Supplementary Materials) without applying patient-specific gray matter masks, which may affect regional accuracy due to anatomical variability. Incorporating individualized segmentation in future work could enhance spatial precision. The cerebellum was not included in our regional analysis, as none of the patients exhibited vasculopathy in the posterior circulation based on MRA and DSA. Another limitation is that we did not account for the effect of sedation on hemodynamics during MR sessions. Sedation significantly impacts hemodynamics by altering heart rate, blood pressure, and vascular resistance,[44] which can vary depending on the type and dosage of sedative administered. A subset of patients required sedation with propofol, which is known to reduce CBF in a dose-dependent manner. Although the same sedation protocol was used for both pre- and postoperative scans in these patients, the vasoconstrictive effects of propofol remain a potential confounder in interpreting absolute CBF values. Investigating these effects in children is challenging because pediatric patients differ widely in age, size, and underlying health conditions, leading to variability in their physiological responses to sedation. Future studies must incorporate stratified sampling based on these intrinsic factors, while following standardized sedation protocols to minimize variability.

Conclusions

This study evaluated vascular hemodynamics using ASL and DSC MRI in a pediatric moyamoya cohort. We observed that bypass surgery leads to increased CBF and decreased transit time in regions affected by vasculopathy. Measurements from ASL and DSC showed a significantly positive correlation across different brain regions. These findings suggest that revascularization may improve vascular hemodynamics in pediatric moyamoya patients and support the application of multi-delay ASL as a non-invasive modality for characterizing CBF and transit time in this population.

Funding

The author(s) disclosed receipt of the following financial support for the research, authorship, and/or publication of this article: This work is supported in part by the American Heart Association Second Century Early Faculty Independence Award #23SCEFIA1141920 (MYZ), Stanford Maternal & Child Health Research Institute Pilot Grant (MYZ), and funding from Bernard and Ronni Lacroute (GKS), the William Randolph Hearst Foundation (GKS) and The Reddy Lee Family Moyamoya Research Fund (GKS).

Acknowledgements

The authors thank Young Chang, Elyssa McFadden, Mark Golchehreh, Aaron Hall, Teresa E. Bell-Stephens, Amber Chan, Joli Vavao, Tuan Duong, Christine Plant, and Jeanne Gu for their technical support, manuscript editing, and project management.

Declaration of conflicting interests

The author(s) declared the following potential conflicts of interest with respect to the research, authorship, and/or publication of this article: Gary Steinberg is a consultant for SanBio, Zeiss, and Surgical Theater, and receives royalties from Peter Lazic, US. These potential conflicts of interest are unrelated to the current study.

Authors' contributions

Moss Y Zhao: conceptualization, methodology, writing, funding acquisition
Sasha Alexander: data curation, project management

Chris Antonio Lopez: data curation
Helena Zhang: data curation
Gabriella Morton: project management
Rui Duarte Armindo: methodology
Kristen W Yeom: image interpretation
Elizabeth Tong: image interpretation
Bruno Passebon Soares: image interpretation, manuscript revision
Sara Lee: patient enrollment, funding acquisition
Michael Moseley: funding acquisition, supervision
Gary K Steinberg: conceptualization, patient enrollment, manuscript revision, funding acquisition, supervision

Supplementary material

Supplemental material for this article is available online.

ORCID iDs

Moss Y Zhao https://orcid.org/0000-0002-0210-7739
Gabriella Morton https://orcid.org/0009-0005-9884-3069
Sarah Lee https://orcid.org/0000-0002-8821-6636
Michael Moseley https://orcid.org/0000-0002-9163-8741
Gary K Steinberg https://orcid.org/0000-0001-6374-1058

References

1. Hara S, Kikuta J, Takabayashi K, et al. Decreased diffusivity along the perivascular space and cerebral hemodynamic disturbance in adult moyamoya disease. *J Cereb Blood Flow Metab* 2024; 44: 1787–1800.
2. Morshed RA, Abla AA, Murph D, et al. Clinical outcomes after revascularization for pediatric moyamoya disease and syndrome: a single-center series. *J Clin Neurosci* 2020; 79: 137–143.
3. Teo M, Abhinav K, Bell-Stephens TE, et al. Short- and long-term outcomes of moyamoya patients post-revascularization. *J Neurosurg* 2022; 1: 1–11.
4. Zhao MY, Armindo RD, Gauden AJ, et al. Revascularization improves vascular hemodynamics – a study assessing cerebrovascular reserve and transit time in moyamoya patients using MRI. *J Cereb Blood Flow Metab* 2023; 43: 138–151.
5. Fan Audrey P, Khalighi Mohammad M, Guo J, et al. Identifying hypoperfusion in moyamoya disease with arterial spin labeling and an [15O]-water positron emission tomography/magnetic resonance imaging normative database. *Stroke* 2019; 50: 373–380.
6. Abhinav K, Furtado SV, Nielsen TH, et al. Functional outcomes after revascularization procedures in patients with hemorrhagic moyamoya disease. *Neurosurgery* 2020; 86: 257–265.
7. Ogoh S. Relationship between cognitive function and regulation of cerebral blood flow. *J Physiol Sci* 2017; 67: 345–351.
8. Weijs RWJ, Shkredova DA, Brekelmans ACM, et al. Longitudinal changes in cerebral blood flow and their relation with cognitive decline in patients with dementia: Current knowledge and future directions. *Alzheimers Dement* 2023; 19: 532–548.
9. van Dinther M, Hooghiemstra AM, Bron EE, et al. Lower cerebral blood flow predicts cognitive decline in patients with vascular cognitive impairment. *Alzheimers Dement* 2024; 20: 136–144.
10. Wang J, Alsop DC, Song HK, et al. Arterial transit time imaging with flow encoding arterial spin tagging (FEAST). *Magn Reson Med* 2003; 50: 599–607.
11. Tsujikawa T, Kimura H, Matsuda T, et al. Arterial transit time mapping obtained by pulsed continuous 3D ASL imaging with multiple Post-Label delay acquisitions: comparative study with PET-CBF in patients with chronic occlusive cerebrovascular disease. *Plos One* 2016; 11: e0156005.
12. Østergaard L. Principles of cerebral perfusion imaging by bolus tracking. *J Magn Reson Imaging* 2005; 22: 710–717.
13. Lin Y-H, Kuo M-F, Lu C-J, et al. Standardized MR perfusion scoring system for evaluation of sequential perfusion changes and surgical outcome of moyamoya disease. *AJNR Am J Neuroradiol* 2019; 40: 260–266.
14. Huang A, Lee C-W and Liu H-M. Time to peak and full width at half maximum in MR perfusion: valuable indicators for monitoring moyamoya patients after revascularization. *Sci Rep* 2021; 11: 479.
15. Gopinath G, Aslam M and Anusha P. Role of magnetic resonance perfusion imaging in acute stroke: arterial spin labeling versus dynamic susceptibility contrast-enhanced perfusion. *Cureus* 2022; 14: e23625.
16. Jeong H, Kim PH, Jung AY, et al. Risk of acute kidney injury after contrast-enhanced MRI examinations in a pediatric population. *Eur Radiol* 2025; 35: 4171–4179.
17. Cheeney SHE, Maloney E and Iyer RS. Safety considerations related to intravenous contrast agents in pediatric imaging. *Pediatr Radiol* 2023; 53: 1352–1363.
18. Lindner T, Bolar DS, Achten E, et al. Current state and guidance on arterial spin labeling perfusion MRI in clinical neuroimaging. *Magn Reson Med* 2023; 89: 2024–2047.
19. Alsop DC, Detre JA, Golay X, et al. Recommended implementation of arterial spin-labeled perfusion MRI for clinical applications: a consensus of the ISMRM perfusion study group and the european consortium for ASL in dementia. *Magn Reson Med* 2015; 73: 102–116.
20. Woods JG, Chappell MA and Okell TW. Designing and comparing optimized pseudo-continuous arterial spin labeling protocols for measurement of cerebral blood flow. *NeuroImage* 2020; 223: 117246.
21. Zhao MY, Fan AP, Chen DY-T, et al. Using arterial spin labeling to measure cerebrovascular reactivity in moyamoya disease: insights from simultaneous PET/MRI. *J Cereb Blood Flow Metab* 2022; 42: 1493–1506.
22. World Medical Association. World medical association declaration of Helsinki: ethical principles for medical research involving human subjects. *Jama* 2013; 310: 2191–2194.
23. Steinberg GK and Gooderham PA. Intracranial-extracranial bypass surgery for moyamoya disease. In: Kalani Y, Nakaji P, Spetzler RF (eds) *Neurovascular surgery*. New York: Thieme, 2015, pp. 1156–1171.

24. Clement P, Mutsaerts H-J, Václavů L, et al. Variability of physiological brain perfusion in healthy subjects – a systematic review of modifiers. Considerations for multicenter ASL studies. *J Cereb Blood Flow Metab* 2018; 38: 1418–1437.
25. Chappell MA, Kirk TF, Craig MS, et al. BASIL: a toolbox for perfusion quantification using arterial spin labelling. *Imaging Neurosci* 2023; 1: 1–16.
26. Zhao MY, Tong E, Duarte Armindo R, et al. Short- and long-term MRI assessed hemodynamic changes in pediatric moyamoya patients after revascularization. *J Magn Reson Imaging* 2024; 59: 1349–1357.
27. Zhao MY, Mezue M, Segerdahl AR, et al. A systematic study of the sensitivity of partial volume correction methods for the quantification of perfusion from pseudo-continuous arterial spin labeling MRI. *NeuroImage* 2017; 162: 384–397.
28. Lansberg MG, Lee J, Christensen S, et al. RAPID automated patient selection for reperfusion therapy. *Stroke* 2011; 42: 1608–1614.
29. Smith SM, Jenkinson M, Woolrich MW, et al. Advances in functional and structural MR image analysis and implementation as FSL. *Neuroimage* 2004; 23 Suppl 1: S208–S219.
30. Desikan RS, Ségonne F, Fischl B, et al. An automated labeling system for subdividing the human cerebral cortex on MRI scans into gyral based regions of interest. *NeuroImage* 2006; 31: 968–980.
31. Smirnov N. Table for estimating the goodness of fit of empirical distributions. *Ann Math Statist* 1948; 19: 279–281.
32. Rao VL, Prolo LM, Santoro JD, et al. Acetazolamide-challenged arterial spin labeling detects augmented cerebrovascular reserve after surgery for moyamoya. *Stroke* 2022; 53: 1354–1362. STROKEAHA.121.036616.
33. Liu P, Liu G, Pinho MC, et al. Cerebrovascular reactivity mapping using resting-state BOLD functional MRI in healthy adults and patients with moyamoya disease. *Radiology* 2021; 299: 419–425.
34. Taki Y, Hashizume H, Sassa Y, et al. Gender differences in partial-volume corrected brain perfusion using brain MRI in healthy children. *NeuroImage* 2011; 58: 709–715.
35. Bolar DS, Gagoski B, Orbach DB, et al. Comparison of CBF measured with combined velocity-selective arterial spin-labeling and pulsed arterial spin-labeling to blood flow patterns assessed by conventional angiography in pediatric moyamoya. *AJNR Am J Neuroradiol* 2019; 40: 1842–1849.
36. Hernandez-Garcia L, Aramendía-Vidaurreta V, Bolar DS, et al. Recent technical developments in ASL: a review of the state of the art. *Magn Reson Med* 2022; 88: 2021–2042.
37. Shiroishi MS, Castellazzi G, Boxerman JL, et al. Principles of T2 *-weighted dynamic susceptibility contrast MRI technique in brain tumor imaging. *J Magn Reson Imaging* 2014; 00: 296–313.
38. Calamante F, Christensen S, Desmond PM, et al. The physiological significance of the time-to-maximum (tmax) parameter in perfusion MRI. *Stroke* 2010; 41: 1169–1174.
39. Seo YS, Lee S, Choi YH, et al. Monitoring posterior cerebral perfusion changes with dynamic susceptibility contrast-enhanced perfusion MRI after anterior revascularization surgery in pediatric moyamoya disease. *Korean J Radiol* 2023; 24: 784–794.
40. Lee M, Zaharchuk G, Guzman R, et al. Quantitative hemodynamic studies in moyamoya disease. *FOC* 2009; 26: E5.
41. Newbould RD, Skare ST, Jochimsen TH, et al. Perfusion mapping with multiecho multishot parallel imaging EPI. *Magn Reson Med* 2007; 58: 70–81.
42. Qin Q, Alsop DC, Bolar DS, ISMRMPerfusion Study Group, et al. Velocity-selective arterial spin labeling perfusion MRI: a review of the state of the art and recommendations for clinical implementation. *Magn Reson Med* 2022; 88: 1528–1547.
43. Scott RM and Smith ER. Moyamoya disease and moyamoya syndrome. *N Engl J Med* 2009; 360: 1226–1237.
44. Koroglu A, Demirbilek S, Teksan H, et al. Sedative, haemodynamic and respiratory effects of dexmedetomidine in children undergoing magnetic resonance imaging examination: preliminary results. *Br J Anaesth* 2005; 94: 821–824.